Semi-blind DFE for MIMO Optical Communications

Kabiru N. Aliyu, Azzedine Zerguine
EE Department and IRC-CSS,
KFUPM,
Dhahran, 31261, KSA
{g201705110, azzedine}@kfupm.edu.sa

Karim Abed-Meraim
Univ. of Orléans / IUF Member
PRISME Lab.,
Orléans, France
karim.abed-meraim@univ-orleans.fr

Linh Trung Nguyen
AVITECH Institute,
VNU Uni.,
Hanoi, Vietnam
linhtrung@vnu.edu.vn

***Abstract*—In the last decade, the coherent transmission over fiber has attracted many research interests, mainly for long-haul transmission, due to its advantages in terms of DSP processing. However, with the raise of demand for higher baud-rates and increased technical requirements, the current DSP algorithms have failed to offer suitable performance in the extreme transmission scenarios such as high State-of-Polarization (SOP) frequencies. Meanwhile, the joint effect of polarization mode dispersion (PMD), fast SOP rotation, carrier frequency offset (CFO) and phase noise significantly degrade the performance of the whole system. In this scenario, the use of conventional blind equalizers such as constant modulus algorithms (CMA) and multi-modulus algorithms (MMA) would not be enough for symbol detection. In this work, we propose the decision feedback estimation (DFE) as the baseline for a joint Multiple-Input Multiple-Output (MIMO) equalization and CFO compensation. The devised DFE-like algorithm, implemented in an adaptive manner, allows MIMO equalization even at high CFO and SOP rates. The algorithm is developed in both blind and semi-blind scenarios based on QAM using the probabilistic constellation shaping (PCS) technique.**

***Index Terms*—Optical Coherent Communications, Semi-blind Equalization, Decision Feedback, Carrier Frequency Offset, SOP**

I. Introduction

Coherent transmission has recently demonstrated significant success in fiber optic communications due to its lower complexity, high performance and capability to achieve high baud rates [1]. Additionally, the information rate in the optical communication systems have improved tremendously close to Shannon's theoretical limits, thanks to the integration of probabilistic constellation shaping (PCS) in coherent transmission [2], [3]. However, the non-uniform symbol distribution in PCS presents more challenges in the phase and frequency estimation process compared to the traditional square Quadrature Amplitude Modulation (QAM) scheme. Likewise, the presence of high State-of-Polarization (SOP) rates, polarization mode dispersion (PMD) and carrier frequency offset (CFO) in the optical communication systems created severe performance impairments, which are mitigated using appropriate DSP algorithms [4]. Furthermore, other optical system impairment factors, such as polarization-dependent loss (PDL), emerge from in-line optical components such as isolators, multiplexers, couplers and amplifiers remain a significant bottleneck challenge for the system.

In long-haul optical communication systems, PDL, chromatic dispersion (CD) and fiber loss are among the static impairments. The PDL and CD can be compensated using the static equalization approach in the frequency domain, where the fiber loss can be addressed using Erbium-Doped Fiber Amplifier in each fiber span [5]. Subsequently, the effect of PDL on the optical signals increases with the length of the fiber. This effect introduces an asymmetry in the Optical Signal-to-Noise ratio (OSNR) between the two polarization states, which results in degradation of the bit error rate (BER), potentially leading to reduced transmission reliability [6]. On the other hand, dynamic impairment usually occurs as a result of SOP and PMD. These impairments are considered the most challenging aspect and require an advanced DSP technique for compensation. In transmission links, SOP might display a variation of $45,000$ rotations/seconds [7] where PMD creates crosstalk along the two polarizations [8].

Essentially, the most crucial equalization techniques considered in coherent detection are pilot-based and blind equalization [9]. Pilot-based equalization requires a training sequence that consumes extra bandwidth, whereas blind equalization relies on statistical information of the transmitted symbols and does not require additional bandwidth [10], [11]. However, to improve the blind equalization performance with less complexity, semi-blind equalization is adopted [12]. Nevertheless, polarization demultiplexing has been presented in the literature [13]–[15] and reference therein. Authors in [13] proposed a fractionally spaced equalizer (FSE) for the mitigation of chromatic dispersion (CD) and PMD in coherent optical communications. Alternatively, authors in [16] proposed an adaptive tracking using an extended Kalman filter for polarization demultiplexing of complex-modulated signals in Stokes space, where the proposed approach displays a robust performance compared to the geometrical approach. However, the Constant Modulus Algorithm (CMA) [14], the Multi-Modulus Algorithm (MMA) [17]–[19], and the Decision-Directed Least Mean Square (DD-LMS) Algorithm [20] are the most frequently used algorithms for multiple-input multiple-output (MIMO) coherent detection. Authors in [14] proposed a constant modulus algorithm (CMA) equalization using a two by two matrix in the digital domain. Similarly, authors in [15] considered a QPSK and 16-QAM modulation schemes,

proposing a blind equalization technique based on independent component analysis to eliminate PMD and PDL. To further improve the receiver performance, Semi-blind solutions that are based on pilots insertion in the frame structure have also been proposed in [21], [22].

In this paper, we propose a joint tackling of the SOP and CFO problems using a semi-blind DFE equalizer as the baseline approach for MIMO optical communication systems. Our adaptive DFE approach enables robust MIMO equalization, even under high CFO and SOP conditions. The proposed algorithm is formulated for both blind and semi-blind scenarios, leveraging QAM and employing the PCS technique to enhance the performance.

The paper is structured as follows: Section II presents the system model, while Section III presents the formulation of the proposed joint semi-blind DFE equalizer. Section IV presents the simulation results.

II. System modeling

Throughout this paper, we only consider linear impairments from signal transmission along the optical fiber. We assume that a static equalizer has compensated chromatic dispersion (CD), therefore, after matched filtering with perfect timing synchronization, the discrete-time (dual-polarized) received baseband signal can be modeled as follows:

$$\boldsymbol{x}(k) = \mathscr{F}^{-1}\left\{\boldsymbol{M}(\omega)\cdot\mathscr{F}\left\{\boldsymbol{R}(k)\,\boldsymbol{s}(k)\right\}\right\}\mathrm{e}^{\mathrm{j}(2\pi\Delta f k+\xi(k))}+\boldsymbol{n}(k),$$

where

- $\mathscr{F}\{\cdot\}$ is the Discrete Fourier Transform (DFT) operation;
- $\boldsymbol{s}(k)=[s_1(k),s_2(k)]^{\mathrm{T}}$ represents the transmitted signals, where $s_1(k)$ (resp. $s_2(k)$) denotes the transmitted signal on X-polarization (resp. Y-polarization), respectively. The superscript $(\cdot)^{\mathrm{T}}$ stands for the transpose operator. The iid source signal is generated according to *Maxwell-Boltzmann* distribution [2] given by:

$$P_X(x)=\frac{\exp(-\lambda x^2)}{\sum_{t\in\mathcal{P}}\exp(-\lambda t^2)}, \tag{1}$$

  where $\lambda > 0$ is a scalar that controls the entropy of the source X, denoted by $H(X)$. $\mathcal{P}=\{\pm1,\pm3,...,\pm(D-1)\}$ represents the alphabet set of PS-D-PAM with its probabilistic vector being given by $\boldsymbol{p}=[P_X(1-D),...,P_X(-1),P_X(1),...,P_X(D-1)]^{\mathrm{T}}$. For PS-$D^2$-QAM, whose entropy is given by $2H(X)$, the distribution is given by the probabilistic matrix $\mathbf{Q}=\boldsymbol{p}\boldsymbol{p}^{\mathrm{T}}$, i.e. $P(x+\mathrm{j}y)=P_X(x)P_X(y)$.
- $\boldsymbol{x}(k)=[x_1(k),x_2(k)]^{\mathrm{T}}$ is the received signals, where $x_1(k)$ (resp. $x_2(k)$) stands for the received signal on X-polarization (resp. Y-polarization);
- $\boldsymbol{R}(k)$ describes the time-varying SOP rotation matrix given as:

$$\boldsymbol{R}(k)=\begin{bmatrix}\cos\theta(k) & \mathrm{e}^{-\mathrm{j}\sin\phi(k)}\sin\theta(k)\\ -\mathrm{e}^{\mathrm{j}\sin\phi(k)}\sin\theta(k) & \cos\theta(k)\end{bmatrix} \tag{2}$$

- $\boldsymbol{M}(\omega)$ is the first-order PMD matrix in the frequency domain written as follows:

$$\boldsymbol{M}(\omega)=\begin{bmatrix}\mathrm{e}^{-\mathrm{j}\omega\frac{\Delta\tau}{2}} & 0\\ 0 & \mathrm{e}^{\mathrm{j}\omega\frac{\Delta\tau}{2}}\end{bmatrix} \tag{3}$$

- Δf is the frequency offset between the transmitter laser and the local oscillator;
- $\xi(k)$ denotes the phase noise corresponding to laser line width expressed as a discrete time-varying phase;
- $\boldsymbol{n}(k)=[n_1(k),n_2(k)]^{\mathrm{T}}$ is the additive zero-mean circularly-symmetric complex-valued Gaussian noise, which is independent across polarizations. The In-phase and Quadrature components of the noise are also independent and identically distributed (iid.).

We consider a semi-blind scheme, where N_p pilot symbols are used at the beginning of the transmission, then after every d data symbols, one pilot symbol[1] is inserted, periodically to better mitigate the frequency jitter.

III. Joint Semi-blind DFE Equalizer

A. Batch DFE

In the absence of CFO, a DFE equalizer consists of two linear filters: a causal filter of length L_B applying to estimated symbols after decision and an anti-causal filter of length L_A+1 applied to the received symbols, where 2×2 taps are hereinafter referred to as $\boldsymbol{B}(k)$ and $\boldsymbol{A}(k)$, respectively. The cost function of DFE is given by.

$$J(\boldsymbol{C})=\mathbb{E}\left\{\left\|\boldsymbol{s}(k)-\boldsymbol{C}^H\boldsymbol{Z}(k)\right\|^2\right\}, \tag{4}$$

where $\mathbb{E}\{\cdot\}$ denotes the expectation operator, the $2(L_A+L_B+1)\times2$ dimensional[2] filter $\boldsymbol{C}$ is given by $\boldsymbol{C}=[\boldsymbol{A}^T,\boldsymbol{B}^T]^T$ where $\boldsymbol{A}=[\boldsymbol{A}^T(0),\cdots,\boldsymbol{A}^T(L_A)]^T$ and $\boldsymbol{B}=[\boldsymbol{B}^T(1),\cdots,\boldsymbol{B}^T(L_B)]^T$, $\|\cdot\|$ denotes the Euclidean norm and $(\cdot)^H$ stands for Hermitian transpose operator. $\boldsymbol{Z}$ is the input to the equalizer, given by

$$\boldsymbol{Z}(k)=\left[\boldsymbol{X}^T(k),\boldsymbol{S}^T(k)\right]^T, \tag{5}$$

where $\boldsymbol{X}(k)=\left[\boldsymbol{x}^T(k+L_A),\boldsymbol{x}^T(k+L_A-1),...,\boldsymbol{x}^T(k)\right]^{\mathrm{T}}$ and $\boldsymbol{S}(k)=\left[\boldsymbol{s}^T(k-1),\boldsymbol{s}^T(k-2),...,\boldsymbol{s}^T(k-L_B)\right]^{\mathrm{T}}$, with $\boldsymbol{s}$ being either a pilot symbol or a previously detected symbol. By letting $\nabla J(\boldsymbol{C})=0$ and after some straightforward derivation, we have

$$\boldsymbol{C}=\mathbb{E}\left\{\boldsymbol{R}_{ZZ}^{-1}\boldsymbol{R}_{Zs}\right\}, \tag{6}$$

$$\boldsymbol{R}_{Zs}=\mathbb{E}\left\{\boldsymbol{Z}(k)\,\boldsymbol{s}^H(k)\right\}, \tag{7}$$

and

$$\boldsymbol{R}_{ZZ}=\mathbb{E}\left\{\boldsymbol{Z}(k)\,\boldsymbol{Z}^H(k)\right\}. \tag{8}$$

[1]As stated, in our simulations, we used one pilot symbol but, obviously, one can use instead small blocks (with several symbols) of pilots, periodically.

[2]In this paper, we used $L_A=L_B$ in all simulation experiments.

B. Adaptive DFE

Replacing $\mathbb{E}\{\cdot\}$ by the exponential window averaging, the adaptive DFE algorithm takes the following form:

$$\hat{\boldsymbol{s}}(k) = \boldsymbol{C}^H(k-1)\,\boldsymbol{Z}(k), \tag{9}$$

$$\boldsymbol{C}(k-1) = \boldsymbol{R}_{ZZ}^{-1}(k-1)\,\boldsymbol{R}_{Zs}(k-1), \tag{10}$$

where

$$\boldsymbol{R}_{ZZ}(k) = \beta\boldsymbol{R}_{ZZ}(k-1) + (1-\beta)\,\boldsymbol{Z}(k)\,\boldsymbol{Z}^H(k), \tag{11}$$

$$\boldsymbol{R}_{Zs}(k) = \beta\boldsymbol{R}_{Zs}(k-1) + (1-\beta)\,\boldsymbol{Z}(k)\,\boldsymbol{s}^H(k), \tag{12}$$

and $0 < \beta \leq 1$ being a chosen forgetting factor. Using the matrix inversion lemma and after straightforward derivation, we get

$$\boldsymbol{R}_{ZZ}^{-1}(k) = \frac{1}{\beta}\Big(\boldsymbol{R}_{ZZ}^{-1}(k-1) - \frac{(1-\beta)\,\boldsymbol{h}(k)\,\boldsymbol{h}^H(k)}{\beta + (1-\beta)\,\boldsymbol{Z}^H(k)\,\boldsymbol{h}(k)}\Big),$$

with

$$\boldsymbol{h}(k) = \boldsymbol{R}_{ZZ}^{-1}(k-1)\,\boldsymbol{Z}(k). \tag{13}$$

Using the latter equations into (10), we can get the adaptive DFE algorithm as summarized in Algorithm 1.

Algorithm 1 Adaptive DFE: At time instant k, do

$\boldsymbol{\epsilon}(k-1) = \boldsymbol{s}(k-1) - \hat{\boldsymbol{s}}(k-1)$
$\boldsymbol{h}(k-1) = \boldsymbol{R}_{ZZ}^{-1}(k-2)\,\boldsymbol{Z}(k-1)$
$\gamma(k-1) = \frac{1-\beta}{\beta+(1-\beta)\boldsymbol{Z}^H(k-1)\boldsymbol{h}(k-1)}$
$\boldsymbol{R}_{ZZ}^{-1}(k-1) = \frac{1}{\beta}\left(\boldsymbol{R}_{ZZ}^{-1}(k-2) - \gamma(k-1)\boldsymbol{h}(k-1)\boldsymbol{h}^H(k-1)\right)$
$\boldsymbol{C}(k-1) = \boldsymbol{C}(k-2) + \gamma(k-1)\,\boldsymbol{h}(k-1)\,\boldsymbol{\epsilon}^H(k-1)$
$\hat{\boldsymbol{s}}(k) = \boldsymbol{C}^H(k-1)\,\boldsymbol{Z}(k)$

Note that $\boldsymbol{s}(k)$ denotes either a pilot symbol if available at time k, or a decided symbol using soft or hard decision [23].

C. Joint DFE and CFO mitigation

The CFO is modeled as a time-varying phase term and the considered cost function that can be written as follows:

$$J'\left(\boldsymbol{C}, \Delta\hat{f}\right) = \mathbb{E}\left\{\left\|\boldsymbol{s}(k)\,\mathrm{e}^{\mathrm{j}2\pi\Delta\hat{f}k} - \boldsymbol{C}^H\boldsymbol{Z}(k)\right\|^2\right\}, \tag{14}$$

where $\Delta\hat{f}$ denotes the estimated frequency of CFO. Since we need to estimate both $\Delta\hat{f}$ and $\boldsymbol{C}$, it is a nonlinear optimization problem. Thus, we propose to optimize the two parameters alternately and iteratively, where $\boldsymbol{C}$ is updated through a block-wise processing presented by Eq. (6) and $\Delta\hat{f}$ is computed by:

$$\arg\max_{f}\,\mathscr{F}\left\{s^H(k)\,\hat{s}(k)\right\}(f). \tag{15}$$

This process is initialized with the N_p pilot symbols in a batch way. In the adaptive scheme, one can simply use the adaptive DFE together with a gradient-based technique to track, if necessary[3], the variations of the CFO. The schematic diagram of the joint DFE and CFO estimation is presented in Fig. 1.

[3]In this work, we considered a constant CFO, in the simulation results.

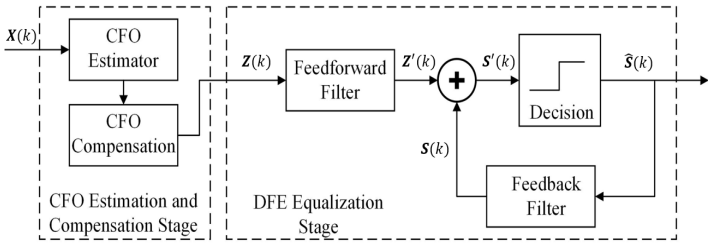

Fig. 1. Schematic diagram of joint DFE and CFO estimation.

D. Simplified DFE

The matrix inversion in the DFE represents the most expensive calculation of the algorithm (in the batch implementation, it costs approximately, $O(L^3)$ where $L = L_A + L_B$ is the equalizer filter size). To reduce this cost, one can take advantage of the whiteness of the input signal (i.e. $R_{SS} = \mathbb{E}(\mathbf{S}(k)\mathbf{S}^H(k)) = \sigma_s^2\mathbf{I}$ ($\mathbf{I}$ being the identity matrix), to derive a simplified version of the algorithm as follows. Based on (7) and (8), $\boldsymbol{R}_{ZZ}$ and $\boldsymbol{R}_{Zs}$ can be rewritten, respectively, as:

$$\boldsymbol{R}_{ZZ} = \begin{bmatrix}\boldsymbol{R}_{XX} & \boldsymbol{R}_{XS}\\ \boldsymbol{R}_{XS}^H & \sigma_S^2\mathbf{I}\end{bmatrix}, \tag{16}$$

$$\boldsymbol{R}_{Zs} = \begin{bmatrix}\boldsymbol{R}_{Xs}\\ \mathbf{0}\end{bmatrix}. \tag{17}$$

Using the inversion lemma of 2×2 block matrices, one can express

$$\boldsymbol{R}_{ZZ}^{-1} = \begin{bmatrix}\boldsymbol{U}^{-1} & \frac{1}{\sigma_S^2}\boldsymbol{U}^{-1}\boldsymbol{R}_{XS}\\ -\frac{1}{\sigma_S^2}\boldsymbol{R}_{XS}^H\boldsymbol{U}^{-1} & \frac{1}{\sigma_S^2}\left(\mathbf{I} + \frac{1}{\sigma_S^2}\boldsymbol{R}_{XS}^H\boldsymbol{U}^{-1}\boldsymbol{R}_{XS}\right)\end{bmatrix}, \tag{18}$$

where

$$\boldsymbol{U} = \boldsymbol{R}_{XX} - \frac{1}{\sigma_S^2}\boldsymbol{R}_{XS}\boldsymbol{R}_{XS}^H. \tag{19}$$

This finally leads to:

$$\boldsymbol{C} = \begin{bmatrix}\boldsymbol{U}^{-1}\boldsymbol{R}_{Xs}\\ -\frac{1}{\sigma_S^2}\boldsymbol{R}_{XS}^H\boldsymbol{U}^{-1}\boldsymbol{R}_{Xs}\end{bmatrix}. \tag{20}$$

This latter formulation helps in reducing the algorithm's cost from $0(L^3)$ to approximately $0((L/2)^3)$ flops. Similarly, in the adaptive scheme[4], one can exploit equation (18) with equations (11) and (12) to derive a reduced cost version of the adaptive DFE algorithm which will be presented in an extended version of this paper.

IV. Simulation Results

This section presents the performance evaluation of the proposed joint semi-blind DFE equalizer for MIMO systems in the context of optical communications. The assessment is based on the Bit-Error Rate (BER), which measures the effectiveness of the proposed joint equalizer in compensation for the CFO and tracks the SOP rate presence in the system.

[4]This is not presented here due to space limitation.

TABLE I
SIMULATION PARAMETERS.

Parameter	Notation & Value
Constellation type	PCS-16-QAM
Entropy of source	$H = 2, 2.5, 3$
Oversampling factor	2
Rolloff factor	0.05
Baud rate	96 GBaud
Initial θ of SOP	$\pi/12$
Initial ϕ of DGD	$\pi/6$
SOP rotation rate (rad/s)	2M (rad/sec)
Number of PMD stages	5
Number of data symbols	$N_s = 18000$
Number of initial pilot symbols	$N_p = 200$
Number of transmitters	$N_t = 2$
Number of receivers	$N_r = 2$
Order of channel	$M = 10$
Forgetting factor	$\beta = 0.998$
Number of Monte-Carlo runs	$M_0 = 50$
Number of iterations for CFO estimation	$N_0 = 20$

The transmitted signal is modulated based on the PCS-16-QAM scheme, and the remaining simulation parameters are given in Table I unless otherwise stated.

The first experiment evaluates the performance of the proposed joint semi-blind DFE equalizer under static and dynamic channel conditions. The static channel scenario (SCN) represents a time-invariant channel with no SOP rotation and first-order PMD, tested with CFOs of 100 MHz. In contrast, the dynamic channel scenario (DCN) includes SOP rotations of 2 Mrad/sec, second-order PMD with two stages and higher-order PMD with five stages at 100 MHz CFO, illustrating a more challenging transmission environment.

The results demonstrate that the proposed joint semi-blind DFE algorithm effectively tracks the SOP rotations and compensates for the CFO. Additionally, it is observed that a slight increase of the OSNR can compensate for the performance margin between SCN and DCN, further highlighting the robustness of the proposed joint semi-blind DFE equalization approach (see Fig. 2).

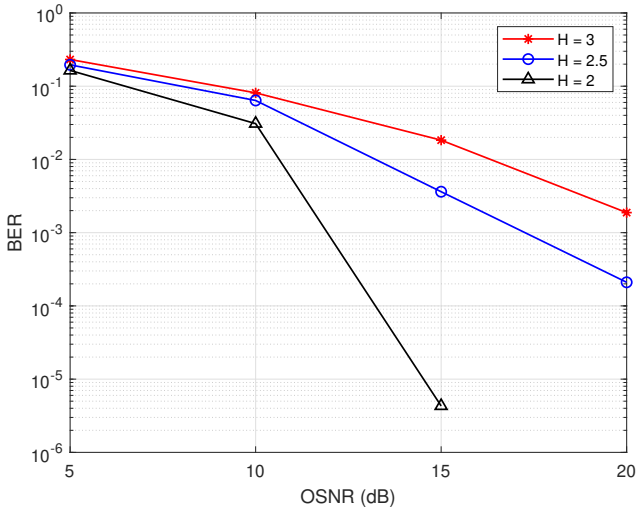

Fig. 3. BER against OSNR for PCS-16-QAM with different entropy at SOP rate = 2 Mrad/sec.

The second experiment, shown in Fig. 3, investigates the impact of PCS entropy (H) on the performance of the proposed joint semi-blind DFE under dynamic conditions with a high CFO of 200 MHz and an SOP rate of 2 Mrad/sec. This creates a highly challenging scenario for SOP rotation tracking and CFO compensation. The results demonstrate that as the entropy H of the PCS-modulated signal decreases, the performance of the joint semi-blind DFE equalizer improves significantly. This decrease in the PCS entropy H optimizes the probability distribution of the transmitted symbols, favoring low-energy symbols that are less sensitive to nonlinear impairments, hence improving equalization efficiency.

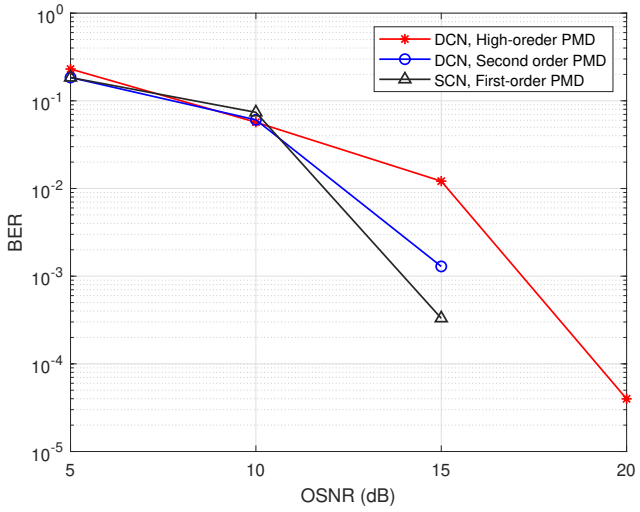

Fig. 2. BER against OSNR for PCS-16-QAM performance, $H = 2.5$.

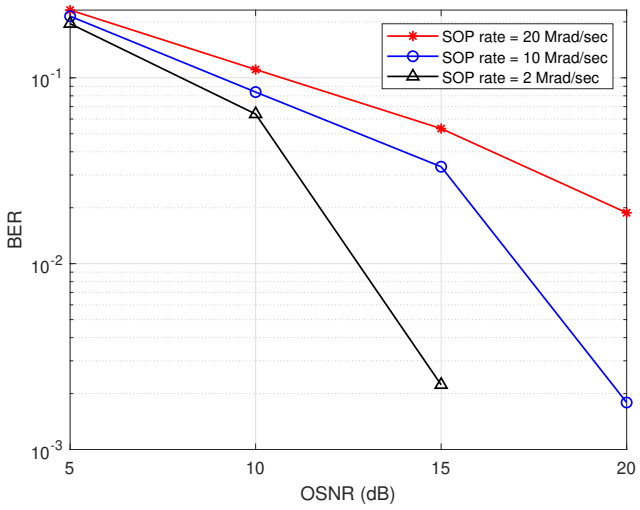

Fig. 4. BER against OSNR for PCS-16-QAM with $H = 2.5$ at different SOP rates.

Figure 4 illustrates the performance comparison for different SOP rotation rates, with a CFO of 200 MHz and a PCS entropy $H = 2.5$. The results indicate that the proposed semi-blind DFE effectively compensates for CFO and tracks SOP rotations of 2 Mrad/sec and 10 Mrad/sec. However, as the SOP rotation rate increases to 20 Mrad/sec, the system requires a minimum of 12 dB OSNR to track the SOP and compensate the CFO. This shows that the dynamic impairment increases at higher SOP rotation rates, making equalization more challenging at moderate and low OSNR levels. Furthermore, the performance can be improved by decreasing the PCS entropy, which helps to optimize the probability distribution of the transmitted symbols.

V. Conclusion

The combined impact of PMD, fast SOP rotation, and CFO presents significant challenges to conventional blind equalizers like CMA and MMA, especially when using PCS modulations. To address these limitations, we propose a decision feedback estimation (DFE)-based approach for joint MIMO equalization and CFO compensation. The latter is of, relatively, low cost and the adaptive DFE algorithm demonstrates robust performance, enabling effective symbol detection even under high CFO and SOP rates.

Acknowledgment

The authors would like to acknowledge the support provided by the Deanship of Research Oversight and Coordination at King Fahd University of Petroleum & Minerals for funding under the Interdisciplinary Research Center for Communication Systems and Sensing through project No. **INCS2404**.

References

[1] K. Kikuchi, "Fundamentals of coherent optical fiber communications," *Journal of lightwave technology*, vol. 34, no. 1, pp. 157–179, 2015.

[2] Z. Qu and I. B. Djordjevic, "On the probabilistic shaping and geometric shaping in optical communication systems," *IEEE Access*, vol. 7, pp. 21454–21464, 2019.

[3] E. M. Liang and J. M. Kahn, "Probabilistic shaping distributions for optical communications," *Journal of Lightwave Technology*, 2025.

[4] S. J. Savory, "Digital filters for coherent optical receivers," *Optics express*, vol. 16, no. 2, pp. 804–817, 2008.

[5] H. Xu, X. Zhang, X. Tang, C. Bai, L. Xi, W. Zhang, and H. Zheng, "Joint scheme of dynamic polarization demultiplexing and pmd compensation up to second order for flexible receivers," *IEEE Photonics Journal*, vol. 9, no. 6, pp. 1–15, 2017.

[6] N. Cui, X. Zhang, W. Zhang, X. Tang, and L. Xi, "True equalization of polarization-dependent loss in presence of fast rotation of sop," *Applied Sciences*, vol. 10, no. 11, p. 3844, 2020.

[7] P. M. Krummrich and K. Kotten, "Extremely fast (microsecond timescale) polarization changes in high speed long haul wdm transmission systems," in *Optical fiber communication conference*, p. FI3, Optica Publishing Group, 2004.

[8] X. Zhou and C. Xie, *Enabling technologies for high spectral-efficiency coherent optical communication networks*. John Wiley & Sons, 2016.

[9] K. N. Aliyu, A. Lawal, K. Abed-Meraim, and A. Zerguine, "Fast subspace-based semi-blind channel estimation for MIMO-OFDM communications," in *2023 31st European Signal Processing Conference (EUSIPCO)*, pp. 1460–1463, 2023.

[10] A. Lawal, Q. Mayyala, K. Abed-Meraim, N. Iqbal, and A. Zerguine, "Toeplitz structured subspace for multi-channel blind identification methods," *Signal Processing*, vol. 188, p. 108152, 2021.

[11] A. Lawal, K. Abed-Meraim, Q. Mayyala, N. Iqbal, and A. Zerguine, "Blind MMSE equalizer for nonlinear SIMO systems," in *2021 18th International Multi-Conference on Systems, Signals Devices (SSD)*, pp. 510–513, 2021.

[12] A. Lawal, K. Abed-Meraim, A. Zerguine, N. Linh Trung, and K. Nasiru Aliyu, "Low-cost blind and semi-blind equalizers for nonlinear SIMO systems," *IEEE Access*, vol. 13, pp. 89108–89117, 2025.

[13] E. Ip and J. M. Kahn, "Digital equalization of chromatic dispersion and polarization mode dispersion," *Journal of Lightwave Technology*, vol. 25, no. 8, pp. 2033–2043, 2007.

[14] K. Kikuchi, "Performance analyses of polarization demultiplexing based on constant-modulus algorithm in digital coherent optical receivers," *Optics Express*, vol. 19, no. 10, pp. 9868–9880, 2011.

[15] A. Nafta, P. Johannisson, and M. Shtaif, "Blind equalization in optical communications using independent component analysis," *Journal of Lightwave Technology*, vol. 31, no. 12, pp. 2043–2049, 2013.

[16] N. J. Muga and A. N. Pinto, "Extended kalman filter vs. geometrical approach for stokes space-based polarization demultiplexing," *Journal of Lightwave Technology*, vol. 33, no. 23, pp. 4826–4833, 2015.

[17] K. N. Aliyu, K. Abed-Meraim, A. Zerguine, and A. Lawal, "Semi-blind multi-modulus approach using embedded pilot for MIMO-OFDM communications," in *2024 58th Asilomar Conference on Signals, Systems, and Computers*, pp. 1547–1551, 2024.

[18] C. Yuxin, H. Guijun, Y. Li, Z. Ling, and L. Li, "Mode demultiplexing based on multimodulus blind equalization algorithm," *Optics Communications*, vol. 324, pp. 311–317, 2014.

[19] Q. Mayyala, K. Abed-Meraim, A. Zerguine, and A. Lawal, "Fast multimodulus blind deconvolution algorithms," *IEEE Transactions on Wireless Communications*, vol. 21, no. 11, pp. 9627–9637, 2022.

[20] S. Randel, R. Ryf, A. Sierra, P. J. Winzer, A. H. Gnauck, C. A. Bolle, R.-J. Essiambre, D. W. Peckham, A. McCurdy, and R. Lingle Jr, "6× 56-gb/s mode-division multiplexed transmission over 33-km few-mode fiber enabled by 6× 6 mimo equalization," *Optics Express*, vol. 19, no. 17, pp. 16697–16707, 2011.

[21] O. Rekik, K. N. Aliyu, B. M. Tuan, K. Abed-Meraim, and N. L. Trung, "Fast subspace-based blind and semi-blind channel estimation for MIMO-OFDM systems," *IEEE Transactions on Wireless Communications*, vol. 23, no. 8, pp. 10247–10257, 2024.

[22] B. Liu, C. Gong, J. Cheng, Z. Xu, and J. Liu, "Blind and semi-blind channel estimation/equalization for poisson channels in optical wireless scattering communication systems," *IEEE Transactions on Wireless Communications*, vol. 21, no. 8, pp. 5930–5946, 2022.

[23] R. Hormis and X. Wang, "Iterative equalization with hard and soft decisions for isi-constrained channels," in *2008 IEEE International Conference on Acoustics, Speech and Signal Processing*, pp. 2905–2908, 2008.